

The PENCIL CODE Newsletter

Issue 2022/2

June 15, 2022, Revision: 1.31

Contents

1	The office hour goes hybrid	1
2	PCUM 2022	1
3	PCUM 2023	1
4	New Nature Astronomy paper involving the PENCIL CODE	2
5	Science & code developments	2
5.1	Second order GW solver	2
5.2	Upwinding and/or SLD	3
5.3	Initial time spectra	4
5.4	Using <code>time_integrals.hydro</code>	4
5.5	Issues with the AMD compiler	5
5.6	Memory usage	5
5.7	Developer meetings and code reviewing	5
6	Papers since April 2022	5

1 The office hour goes hybrid

Since June 9, 2022, the office hour went into hybrid mode and we were more people in the office (Figure 1) than on zoom (Figure 2).

2 PCUM 2022

The 18th annual pencil code user meeting (PCUM-22) was held virtually and hosted for the first time in India by the Indian Institute of Astrophysics, Bengaluru from 4–10 May, 2022. Yet another first for this meeting were the introductory lectures for new users of the code. We also had several science talks demonstrating the usefulness of the code. The lectures are now available in the YouTube channel at the link <https://youtube.com/playlist?list=PL1io4hS6YJq29NUA1DkdcHvqMddSXZ8Ko>

whereas, the scientific talks can be accessed at <https://youtube.com/playlist?list=PL1io4hS6YJq2cMn1ive08Po9G19R1U7Y0>.

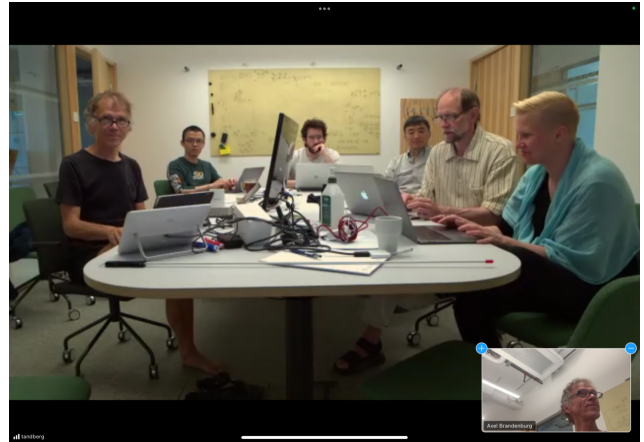


Figure 1: View of the PENCIL CODE *Office* of the office hours.



Figure 2: Hybrid view of the PENCIL CODE *Office*.

More information about pcum-22 is available at <https://t.co/4NOVQNffC1>; see Figure 3 for a group picture and others.

3 PCUM 2023

Already now we are looking forward to the next meeting in 2023, which will be hosted by Vartika Pandey and Johannes Tschernitz from Graz University (which is in the city center!).



Figure 3: Screenshot from Piyali's Twitter page: <https://twitter.com/piyalico/status/1523936663612706819>.

4 New Nature Astronomy paper involving the PENCIL CODE

A new Nature Astronomy paper involving the PENCIL CODE has now appeared. Code owner Wladimir Lyra was co-author (and lead theory author) in Currie *et al.* (2022). In this mainly observational work, an embedded protoplanet was found via direct imaging around the star AB Aurigae, whose properties defy explanation via the core accretion model of planet formation. Wlad used the Pencil Code to construct a model that fits the observational constraints if the competitive theory, gravitational instability, is considered. The in-utero protoplanet, AB Aurigae b, is the first protoplanet candidate for which gravitational instability is plausible. The model was two-dimensional, in cylindrical coordinates, using self-gravity calculated via the method of logarithmic spirals, as im-

plemented in the code in 2017 and in the sample 2d-tests/selfgravdisk-logspirals. See Figure 4 for a comparison between the observational image (left panel) and the intensity calculated with the Pencil Code model (right panel) after post-processing with the radiative transfer code RADMC-3D.

5 Science & code developments

The PCUM22 presented an excellent opportunity to make some progress with the code. Below just a small selection. Some of those developments are already described in the manual.

5.1 Second order GW solver

There have now been over ten papers describing and using the gravitational waves (GWs) solver of the PEN-

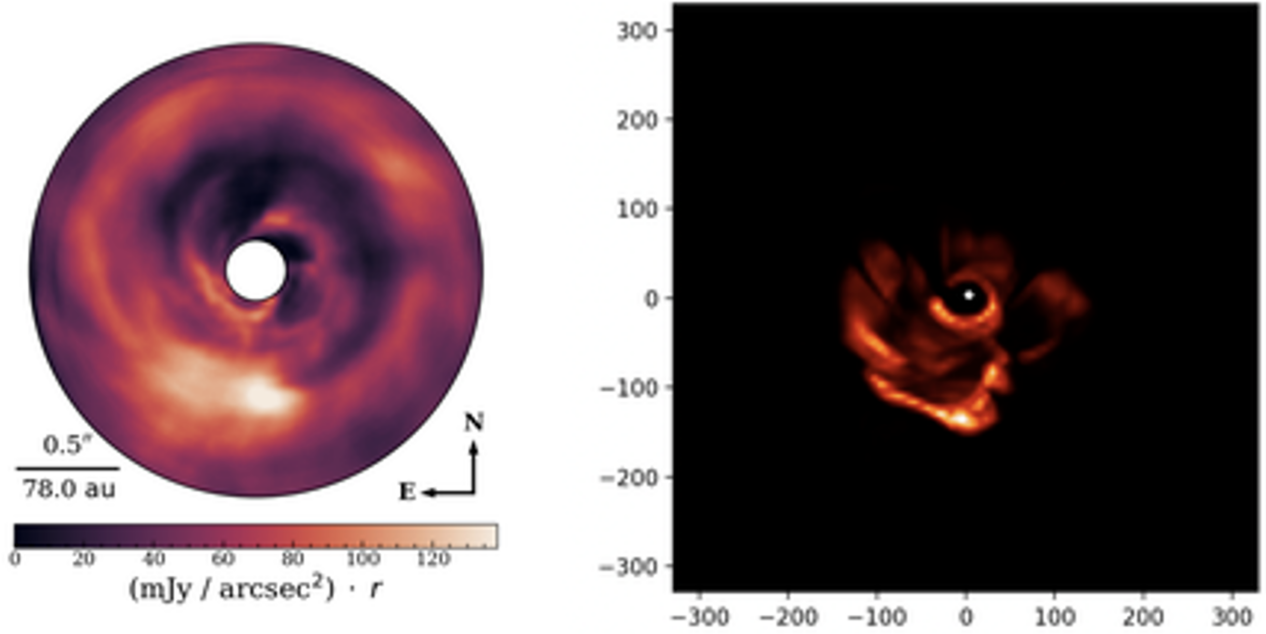


Figure 4: The CHARIS observation Currie *et al.* (2022) (left) and the model intensity calculated with the Monte Carlo radiative transfer code RADMC-3D over a base 2D Pencil Code hydrodynamical simulation (right). The hydro model used the self-gravity logspirals solver.

CIL CODE. By default, we have been assuming the GW source to be constant between two time steps. This implies an accuracy of the GW solution that scales linearly with the time step δt , while the magnetic field, related to the magnetic stress, scales cubically with δt , as expected for our third order Runge-Kutta method. Since the Fourier-transformed source terms $\tilde{T}_{+/\times}$ are being stored in the f -array, it is easy to extract for each wavevector the increment of the stress, $\delta\tilde{T}_{+/\times}$, and to use it in an improved update of the GW field through

$$\tilde{h}_{+/\times} = \dots + \delta\tilde{T}_{+/\times} (1 - \sin \omega \delta t / \omega \delta t), \quad (1)$$

$$\dot{\tilde{h}}_{+/\times} = \dots + \delta\tilde{T}_{+/\times} (1 - \cos \omega \delta t) / \omega^2 \delta t. \quad (2)$$

This more accurate solver is invoked by setting `itorder.GW=2`, which now results in a quadratic scaling of the error of the GW field; see Fig. 5.

5.2 Upwinding and/or SLD

A standard advection experiment is shown in Fig. 6 for $n_x = 128$ mesh points over a 2π domain with advection velocity $U_x = 1$ and diffusivity $\kappa = 10^{-4}$, so $\kappa/U_x \delta x = 0.002$. We see that upwinding causes the wiggles to be slightly stronger.

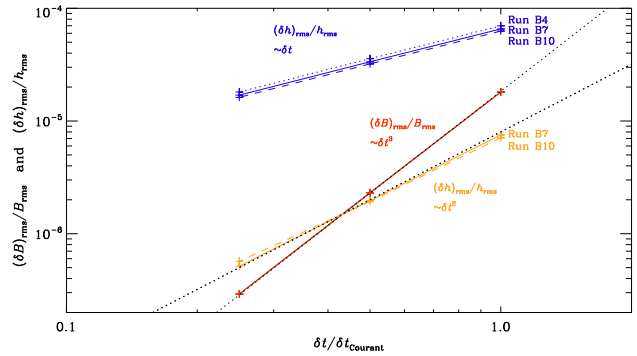


Figure 5: Scalings of the relative error in the magnetic field, $(\delta B)_{\text{rms}}/B_{\text{rms}}$, and the gravitational strain $(\delta h)_{\text{rms}}/h_{\text{rms}}$ for GWs generated by the chiral magnetic effect, which leads to an exponentially increasing magnetic field. Low resolution (32^3) versions of the Runs B4, B7, and B10 of Brandenburg *et al.* (2021, ApJ 911, 110).

In Fig. 7, we compare turbulence simulations with 512^3 mesh points using $\nu = 10^{-4}$, a forcing amplitude $f_0 = 0.02$, and a forcing wavenumber $k_f = 1.5$. The

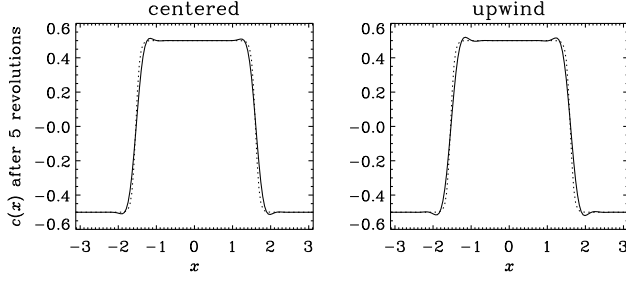


Figure 6: Advection with centered (left) and upwinding (right) schemes with diffusivity $\kappa = 10^{-4}$, $n_x = 128$ mesh points, and an advection velocity of unity.

resulting Mach number is then 0.13 and the Reynolds number is $u_{\text{rms}}/\nu k_f = 900$.

We also show a comparison with a run without regular diffusion, but with slope-limited diffusion (SLD) instead. SLD is a device to help preventing the code from crashing and is routinely used in the MURaM code.¹ However, microphysical viscosity still plays a role, so the question is what is the right mix between SLD and viscous diffusion. SLD was implemented into the PENCIL CODE mainly by Piyali and Jörn.

The colored dashed-dotted lines all use SLD with finite ν . The SLD simulations are all based on the sample `small-scale-dynamo-slope-limited-diffusion` and use `h_sld_visc=1.0` and `nlf_sld_visc=3.0` for the viscosity, i.e., `ivisc='nu-slope-limited'`, and similarly for the density. Without SLD, the smallest viscosity we can use is $\nu = 10^{-4}$. We see that with SLD and $\nu = 0$, the code still works, but there appears to be an artificially enhanced bottleneck. For 5×10^{-5} and 2×10^{-5} , the bottleneck is not yet visibly enhanced, so SLD can be regarded as a device to enhance the Reynolds numbers by factors between 2 and 5, depending on how much of an artifact one is willing to risk.

A reasonable compromise is to lower the non-linear parameter in the momentum equation to `nlf_sld_visc=1.0`. In that case with $\nu = 0$ looks virtually identical to the case with `nlf_sld_visc=3.0` and 5×10^{-5} .

5.3 Initial time spectra

In the past, spectra for the initial time were never written, but now this is possible with `lspec_start=T` in

¹ Rempel, M., “Numerical simulations of quiet sun magnetism: on the contribution from a small-scale dynamo,” *Astrophys. J.* **789**, 132 (2014).

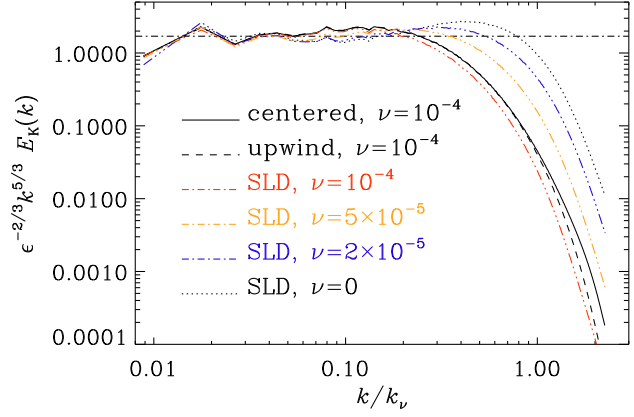


Figure 7: Comparison of centered (solid lines) and upwinding (dashed lines) advection in a 512^3 isothermal turbulence simulation forced with $f_0 = 0.02$ and $\nu = 10^{-4}$. The computational domain is L^3 with $L = 2\pi$ and the forcing wavenumber is $k_f = 1.5$. The dotted line gives a run without regular diffusion, but with SLD instead. The colored dashed-dotted lines all use SLD with finite ν : 10^{-4} (red), 5×10^{-5} (orange), and 2×10^{-5} (blue). The dotted lines are for $\nu = 0$, with two different values of `nlf_sld_visc`.

`run.in` under `run_pars`. When you turn this on, the first *two* times are actually written. This is because with gravitational waves, the transverse-traceless stress spectrum (but not the other gravitational wave spectra) are only available after the first time step, so they are output under the wrong time label. In that case, the initial time has just zeros, and only the next time contains the actual initial spectrum (but marked with the wrong time).

5.4 Using time_integrals_hydro

In Section 4.2 of the PENCIL CODE Newsletter 2021/2, we reported on the calculation of temporal correlation functions during run time. During the Office Hours of June 9, questions about the functionality of this module emerged. Therefore, Hongzhe Zhou from Nordita has reviewed below the essentials of this tool, which is part of the code.

The subroutine needs one or more auxiliary variables, like `uut` or `oot`, and so on. One needs two input variables: A real variable `dtcor`, and a logical variable `ltime_integrals_always`.

`dtcor` sets the resetting time of `uut`. By resetting, we mean setting `uut = uu` at that moment. If `dtcor ≤ 0`, then `uut` will be only reset at the first timestep, i.e.,

it = 1. If `dtcor > 0`, then `uut` will be reset every `dtcor` time units.

`ltime_integrals_always` determines whether we want to integrate `uut` in time. If `True`, this is performed. One can also set some `omega_fourier = ω` , which is by default 0. If non-zero, $\text{uut}(t) = \int_{t_0}^t \text{uu}(t') \cos \omega t' dt'$, and $\text{uust}(t) = \int_{t_0}^t \text{uu}(t') \sin \omega t' dt'$, where t_0 is the last time when `uut` is reset to be equal to `uu`.

5.5 Issues with the AMD compiler

Building the Pencil Code with `flang/clang` and `mpich` fails to produce functional executables. Apart from the known (and soon to be resolved) compilation issue of intolaterated `entry` uses, execution results in segmentation fault, the traceback being useless:

```
address not mapped to object at address (nil))
==== backtrace (tid: 641439) ====
0 0x0000000000012c20 .annobin_sigaction.c()
sigaction.c:0.
```

Building serial code, however, is successful. The used version was 13.0.0. Any experiences and advice are welcome.

5.6 Memory usage

At finishing `run.x`, the code now outputs the maximum memory usage, both per process and in total. However, the numbers do not match by-hand estimates, so cannot be considered reliable at present. The employed system call is `getrusage`, advice again welcome.

5.7 Developer meetings and code reviewing

To disentangle more science- and usage-related discussions from more development-related ones, it was decided during the recent PCUM to offer an additional “developer meeting” on an on-demand basis, but typically once per month. One of the first tasks of the upcoming first meeting at the end of this month will be to form a team, which outlines a scheme for *code reviewing*. In view of the growing complexity of the code and of responsibility towards, in particular, novice users, a majority of the developers agreed that potentially risky commits shall be reviewed in the future before entering the (yet to be defined) “stable branch” of the code. Proposals for the said scheme are requested.

6 Papers since April 2022

As usual, we look here at new papers that make use of the PENCIL CODE. Since the last newsletter of April 5, five new papers have appeared on the arXiv, and eight others, some of which were just preprints and have now been published. We list both here, 13 altogether. A browsable ADS list of all PENCIL CODE papers can be found on: https://ui.adsabs.harvard.edu/user/libraries/iGR7N570Sy6A1hDMQRTe_A. If something is missing in those entries, you can also include it yourself in: <https://github.com/pencil-code/pencil-code/blob/master/doc/citations/ref.bib>, or otherwise just email brandenb@nordita.org. A compiled version of this file is available as <https://github.com/pencil-code/website/blob/master/doc/citations.pdf>, where we also list a total of now 102 code comparison papers in the last section “Code comparison & reference”. Those are not included in our list below, nor among the now total number of 630 research papers that use the PENCIL CODE.

References

- AlbertoRoper, AlbertoRoper/GW_turbulence: v1.0.0, Zenodo 2022.
- Baehr, H., Zhu, Z. and Yang, C.C., Direct Formation of Planetary Embryos in Self-Gravitating Disks. *arXiv e-prints*, 2022, arXiv:2204.13310.
- Brandenburg, A. and Ntormousi, E., Dynamo effect in unstirred self-gravitating turbulence. *Month. Not. Roy. Astron. Soc.*, 2022, **513**, 2136–2151.
- Currie, T., Lawson, K., Schneider, G., Lyra, W., Wisniewski, J., Grady, C., Guyon, O., Tamura, M., Kotani, T., Kawahara, H., Brandt, T., Uyama, T., Muto, T., Dong, R., Kudo, T., Hashimoto, J., Fukagawa, M., Wagner, K., Lozi, J., Chilcote, J., Tobin, T., Groff, T., Ward-Duong, K., Januszewski, W., Norris, B., Tuthill, P., van der Marel, N., Sitko, M., Deo, V., Vievard, S., Jovanovic, N., Martinache, F. and Skaf, N., Images of embedded Jovian planet formation at a wide separation around AB Aurigae. *Nat. Astron.*, 2022.
- Kahniashvili, T., Clarke, E., Stepp, J. and Brandenburg, A., Big Bang Nucleosynthesis Limits and Relic Gravitational-Wave Detection Prospects. *Phys. Rev. Lett.*, 2022, **128**, 221301.

- Käpylä, P.J., Solar-like Dynamos and Rotational Scaling of Cycles from Star-in-a-box Simulations. *Astrophys. J. Lett.*, 2022, **931**, L17.
- Mtchedlidze, S., Domínguez-Fernández, P., Du, X., Brandenburg, A., Kahniashvili, T., O’Sullivan, S., Schmidt, W. and Brüggen, M., Evolution of Primordial Magnetic Fields during Large-scale Structure Formation. *Astrophys. J.*, 2022, **929**, 127.
- Navarrete, F.H., Schleicher, D.R.G., Käpylä, P.J., Ortiz, C. and Banerjee, R., Origin of eclipsing time variations in Post-Common-Envelope binaries: role of the centrifugal force. *arXiv e-prints*, 2022, arXiv:2205.03163.
- Roper Pol, A., Gravitational waves from MHD turbulence at the QCD phase transition as a source for Pulsar Timing Arrays. *arXiv e-prints*, 2022, arXiv:2205.09261.
- Roper Pol, A., Mandal, S., Brandenburg, A. and Kahniashvili, T., Polarization of gravitational waves from helical MHD turbulent sources. *J. Cosmol. Astropart. Phys.*, 2022, **2022**, 019.
- Sharma, R. and Brandenburg, A., Low frequency tail of gravitational wave spectra from hydromagnetic turbulence. *arXiv e-prints*, 2022, arXiv:2206.00055.
- Stejko, A.M., Kosovichev, A.G., Featherstone, N.A., Guerrero, G., Hindman, B.W., Matilsky, L.I. and Warnecke, J., Constraining Global Solar Models through Helioseismic Analysis. *arXiv e-prints*, 2022, arXiv:2204.05207.
- Yang, Y. and Zhu, J.Z., Turbulence compressibility reduction with helicity. *Phys. Fluids*, 2022, **34**, 045113.

This PENCIL CODE Newsletter was edited by Axel Brandenburg <brandenb@nordita.org>, Nordita, KTH Royal Institute of Technology and Stockholm University, SE-10691 Stockholm, Sweden; and Matthias Rheinhardt <matthias.rheinhardt@aalto.fi>, Department of Computer Science, Aalto University, PO Box 15400, FI-00076 Aalto, Finland. See <http://www.nordita.org/~brandenb/pencil-code/newsletter> or <https://github.com/pencil-code/website/tree/master/NewsLetters> for the online version as well as back issues.